

On the entropy devil's staircase in a family of gap-tent maps

Karol Życzkowski
Center for Plasma Research
University of Maryland
College Park, MD 20742

Erik M. Bollt
Mathematics Department
572 Holloway Rd
U.S. Naval Academy
Annapolis, MD 21402-5002.

January 3, 2022

Abstract

To analyze the trade-off between channel capacity and noise-resistance in designing dynamical systems to pursue the idea of communications with chaos, we perform a measure theoretic analysis the topological entropy function of a "gap-tent map" whose invariant set is an unstable chaotic saddle of the tent map. Our model system, the "gap-tent map" is a family of tent maps with a symmetric gap, which mimics the presence of noise in physical realizations of chaotic systems, and for this model, we can perform many calculations in closed form. We demonstrate that the dependence of the topological entropy on the size of the gap has a structure of the devil's staircase. By integrating over a fractal measure, we obtain analytical, piece-wise differentiable approximations of this dependence. Applying concepts of the kneading theory we find the position and the values of the entropy for all leading entropy plateaus. Similar properties hold also for the dependence of the fractal dimension of the invariant set and the escape rate.

PACS: 05.45.+b, 47.52.+j, 47.53.+n, 95.10.Fh

Keywords: Chaos Communication, Topological Entropy, Kneading Theory, Fractal Measure, Devil's staircase, Symbolic Dynamics.

e-mail: ¹karol@chaos.ifuj.edu.pl

²bollt@nadn.navy.mil

Permanent address: Instytut Fizyki im. Smoluchowskiego, Uniwersytet Jagielloński, ul. Reymonta 4, 30-059 Kraków, Poland

1 Introduction

Long term evolution of a chaotic system is, by definition, unpredictable. The topological complexity of a dynamical system has classically been measured in terms of topological entropy [1], which may be considered as the growth rate of distinct states of the dynamical system, to the topic observer. Shannon's information theory tells us that a sequence of events conveys information only if the events are not fully predictable, and therefore, the topological entropy may be considered as a quantitative measurement of the information generating capacity of the chaotic dynamical system [2, 3]. On the other hand, metric-entropy can also be considered as a statistical quantification of irregular behavior, where probability of events are weighted in terms of the specific invariant measure chosen. Indeed, the link between these two types of quantities, topological and metric entropy, is in terms of the choice of invariant measure.

Given this classical and deeply rooted link between chaos and information theory, perhaps it is surprising that only recently we have finally realized that the link can be exploited, since chaotic oscillators can be controlled to transmit messages, [4, 5]. However, such exploitation of chaotic oscillators awaited the (now obvious) realization that chaos is controllable; following the seminal "OGY" paper [6] at the beginning of this decade, there has literally been an explosion of various approaches and wide applications of the concept. The oxymoron between the words, "chaos" and "control," is resolved by the fact that a chaotic dynamical system is deterministic, even while it is long-term unpredictable.

The Hayes et. al. [4] method of chaos communication relies on the now classical description of a chaotic dynamical system in terms of a (semi-)conjugacy (an equivalence) to the Bernoulli-shift map symbolic dynamics [7, 8]. Given the link of a conjugacy function, i.e., a coding function, control of chaotic trajectories is equivalent to control of (message bearing) digital bits. However, there were practical obstacles: 1) experimentally observed chaotic dynamical systems are typically nonhyperbolic [9] and therefore Markov generating partitions are difficult to specify [10, 11], 2) even small channel noise could cause bit-errors. For example, in the case of a two-symbol dynamics representation, a point x near the symbol partition, which bears the message bit, say a 0, may be kicked across the partition by external noise, and therefore an error-bit, a 1, is inadvertently transmitted. One of us has recently co-authored a technique to solve both of these problems [12]. Avoiding neighborhoods of the generating partition, and all pre-iterates of the partition, yields an invariant Cantor-like unstable chaotic saddle, which we showed, is robust to reasonably high noise amplitudes. Interestingly, the topological entropy of these unstable saddles was found to be a monotone nonincreasing devil's staircase-like function of the noise gap widths. In a subsequent work [13], this devil's staircase function was analyzed from a topological standpoint, by a "bifurcation" diagram in s , of the word-bins, which were found to collide with each other at varying s values, thus creating the "at-spots." While we have initially been motivated to study the one-d maps with a gap, due to the communications application, we have subsequently also found the analysis of their ergodic properties to be quite rich.

In this paper, we shall be concerned with ergodic properties of the tent with a gap - a 1D dynamical system defined for $x \in [0;1]$ by [12]

$$f^n(x) = \begin{cases} 2x & \text{for } x \in [0; (1-\epsilon)/2] \\ 1 - \text{gap} & \text{for } x \in ((1-\epsilon)/2; (1+\epsilon)/2) \\ 2(1-x) & \text{for } x \in ((1+\epsilon)/2; 1] \end{cases} \quad (1)$$

where the size of the gap ϵ is a free parameter $0 < \epsilon < 1$. The value of the function inside the gap ($1 - \text{gap}$) is an arbitrary number outside the interval $[0;1]$. See Fig. 1. This map has the desired property that orbits have reduced probability of bit error due to noise of amplitude less than ϵ [12]. For simplified analysis in this paper, we consider these flattened tent maps Eq. (1), for which many calculations are in closed form, and which may be considered to be typical of truncated continuous one-hump maps. The entropy of the closely related trapezoidal maps (at "roof" of the tent instead of the gap) was studied in [14], but their analysis was quite different, involving splitting the family of maps into a codimension-one foliation according to possible dynamical behaviors.

The kneading theory of Thurston and Milnor, introduced in Ref. [15], revealed the importance of the itineraries of the critical points, the so-called kneading sequences, for the admissibility of other itineraries. Kneading theory gives a bifurcation theory of symbol sequences, which for one parameter "full families" of maps, including the logistic map $x_{n+1} = x_n(1 - x_n)$ and the tent map $x_{n+1} = s(1 - 2|x - 1/2|)$. The symbol dynamical representation of bifurcations includes the periodic windows in Sharkovsky's order, and corresponding at-spots on the topological entropy versus parameter value function. "Fully developed chaos" occurs when these maps are everywhere two-to-one ($s > 4$, or $s > 2$); there is a conjugacy to the full shift and the topological entropy is $h_T = \ln(2)$. Correspondingly, the topological entropy is found to be constant in periodic windows [15, 16, 17, 18], which are known to be dense in the parameter for the logistic map, and a closely related, quadratic map [19]. As we shall clarify in this paper, an analogous situation occurs for our model noise-resistant tent gap-map Eq. (1); as the gap parameter ϵ is increased the maximal value of the map is decreased, and correspondingly the kneading sequence is decreased, with now familiar consequences to the topological entropy function, which also has at-spots in the window regions. In fact, staircase like functions can be found repeatedly in the dynamical systems literature [20], and they often signify structural stability of the observed quantity.

A brief overview of this paper is as follows. In Section 2, we will make the necessary introductory definitions and standardize notation, concerning entropy, as well as gap boundaries, and preimages, and relevant measures. In Section 3, we derive conceptually simple and new formulas for the direct computation of the devil's staircase topological entropy function, summarized by Proposition 1. In Section 4, we briefly demonstrate, by example, the efficacy of the formula of Proposition 1. Then in Section 5, we discuss implications to the structure of the devil's staircase function, which we can conclude using the formula, and the closed form representation of the endpoints of the "at-spots." In Section 6, (and Appendix A), we link the roots of the corresponding polynomials to the topological entropy (and we relate this to the kneading theory of Milnor and Thurston [15]). We show how the infinitely nested structure of the devil's staircase function is correspondingly linked to a sequence of "descendant" polynomials, by several operators on sequence space, which we shall discuss. Furthermore, we discuss the structure of the at-spots, in Proposition 2, and we relate this to the familiar Feigenbaum-like accumulation. This leads to several exact statements which can be made concerning values of the entropy at specific points, as well as a sharp estimate for the "maximal" topologically nondegenerate gap, ϵ_c . In Section 7, we discuss a generalization based on weakening the assumptions of Proposition 1, yielding Proposition 3 in which we show that topological entropy of a class of maps can be calculated by "averaging" (with respect to the appropriate measure) the pointwise preimage count. Finally, in Section 8, we discuss implications to the pointwise spectrum of fractal Renyi-dimensions, as well as escape rates.

2 Measures and Entropies of the Tent Gap-Map

Before we may begin our main propositions in the following sections, we have several preliminary definitions and derivations to present in this section.

The topological entropy of a map f on its phase space Y , may be defined in the symbol space representation as the asymptotic rate of growth of permissible words with respect to word length,

$$h_T = \lim_{n \rightarrow \infty} \frac{\ln N(n)}{n}; \quad (2)$$

where $N(n)$ is the number of permissible words of length n . Alternatively, we may define the topological entropy to be

$$h_T = \sup_{\mathcal{M}_1(f)} h(\mu; f); \quad (3)$$

where we take the supremum over entropies with respect to the set of all invariant measures $\mathcal{M}_I(f)$, of f . For a topological Markov chain, such as f , this supremum is actually attained by the entropy with respect to the Parry measure, $h_T(f) = h(\nu; f)$ [21], also known as Parry's topological entropy measure.

The use of formula Eq. (2) requires splitting the phase space $Y = [0; 1]$ into cells of equivalent m -iterate f^m orbits, which we can write in closed form for our model tent map f ; we will use the formula for the m -bit bins extensively throughout the rest of this paper. In fact, our ability to write the m -bit bins A_{mk} in closed form, allows us to explicitly perform many of the calculations in this paper, which was a main motivation of choosing the model Eq. (1). To find the (up to) 2^m , m -bit bins, A_{mk} , consider the critical point $x_c = 1/2$ of the tent map f_0 . It has 2^m m -th preimages with respect to the tent map (without the gap). They are $f_0^{-m}(x_c) = (2k-1)/2^{m+1}$ with $k = 1; 2; \dots; 2^m$. Let A_{01} denote the gap $A_{01} = ((1-\epsilon)/2; (1+\epsilon)/2)$. Its m -th preimages with respect to the system f^m have the width $\epsilon/2^m$ and are centered at the preimages of the critical point. Denoting m th preimages of the gap by A_{mk} we obtain

$$A_{mk} = \left(\frac{2k-1-\epsilon}{2^{m+1}}; \frac{2k-1+\epsilon}{2^{m+1}} \right); \quad (4)$$

where $m = 1; 2; 3; \dots$ and $k = 1; \dots; 2^m$. We note that depending on the size of the gap ϵ some preimages, corresponding to different values of m , may merge together, and it is exactly such overlaps which cause topological entropy at spots. Also note that each of the m -bit word cells A_{mk} are the same length (Lebesgue measured); this is due to the fact that our map f has a constant magnitude slope, $|f'(x)| = 2$.

We also find it useful to consider, ν_{SRB} , the SRB invariant measure for the system f . It may be defined as the eigenmeasure of the Koopman operator associated with the system (i.e. the adjoint to Frobenius-Perron operator) corresponding to the largest eigenvalue. A detailed discussion of these measures can be found in Ref. [22] for "cookie cutters."

Proposition 0: The support of ν_{SRB} is contained in $X = [f^m(y_m); y_m] = [\epsilon/2^m; 1 - \epsilon/2^m]$, where y_m is the maximal value of the system f^m $((1-\epsilon)/2) = 1 - \epsilon/2$, (see Fig. 1).

The support of ν_{SRB} equals $S = \lim_{n \rightarrow \infty} \bigcap_{i=1}^n S_n$, where

$$S_n = \bigcap_{m=0}^n f^{-m}(A_{00}) = \bigcap_{m=0}^n \bigcup_{k=1}^{2^m} A_{mk} \quad (5)$$

Let us also define the uniform measure ν_u , constructed inductively on S as follows:

$$\text{let } \nu_1 \text{ be the uniform measure on } S_1 \text{ normalized so that } \int_X d\nu_1 = 1; \quad (6)$$

$$\text{let } \nu_n \text{ be the uniform normalized measure on } S_n; \quad (7)$$

$$\text{the uniform measure } \nu_u \text{ is defined by the weak limit } \nu_u = \lim_{n \rightarrow \infty} \nu_n; \quad (8)$$

The uniform measure ν_u is connected to the natural measure on stable manifold ν_s , which is often considered in the physical literature [23]. Let us draw randomly, $N(0)$ initial points with respect to the uniform density on the set $Y = [0; 1]$ which contains S , and let $N(n)$ denote the number of points which did not leave the system by the n -th iterate. Let C be any Borel subset of Y , and $N_s(C; n)$ denote the number of initial conditions belonging to C whose trajectories remain in the system for n iterations. Then one defines [23]

$$\nu_s(C) = \lim_{n \rightarrow \infty} \lim_{N(0) \rightarrow \infty} \frac{N_s(C; n)}{N(n)}; \quad (9)$$

Remark for $x \in S$ both measures are proportional, $\nu_u(A) = c \nu_s(A)$, for Borel subsets $A \subset Y$, where the proportionality constant c depends on the choice of the set Y .

For the case of the tent map f , in Eq (1), we can show that the ν_{SRB} , corresponding to natural measure, coincides with the Parry's maximal entropy measure, ν . To show this, we observe that the

absolute value of the derivative is constant: $|f^0(x)| = 2$ for any $x \in Y$. Hence, the topological entropy and the Kolmogorov-Sinai entropy are equal $h_T = h_{KS} = h_q$. The notation h_q denotes the generalized Rényi entropies, which are discussed in detail in [24]. This coincidence follows since the average $\int_Y \ln |f^0(x)| d\mu(x)$ equals $\ln 2$, independently of the measure μ . Hence, we see that the topological pressure, which is defined [22],

$$P(\cdot) = \sup_{\mu} \int_Y \ln |f^0(x)| d\mu(x); \quad (10)$$

where the supremum is taken over all invariant measures of f , has the constant integral fixed at $\ln 2$, for all measures μ . It follows then that supremum is achieved, by the measure which we denote μ_{SRB} , irrespective of the parameter α . Therefore, in this case, it follows that the SRB measure coincides with the maximal entropy measure, $\mu = \mu_{SRB}$.

3 Topological entropy expressed by mean number of preimages

In [12, 13, 25], it was shown that the topological entropy function $h_t(\alpha)$ is a "devil's staircase" function for the model f_α . We are now in a position to better understand the flat spots of the staircase. In this section, we also give a Proposition, which gives an explicit construction to generate a sequence of approximating functions which asymptotically converge to the devil's staircase.

We begin by noting that the point $f_\alpha^2(y_m) = 4\alpha$ divides the support S into two sets: E_2 contains all points $x < 4\alpha$ of the support which have two preimages with respect to f_α , and $E_1 = S \setminus E_2$ consists of points with one preimage only. See Fig. 1.

Let us define a function $M(\alpha)$

$$M(\alpha) = \frac{\mu_{\alpha}(E_2)}{\mu_{\alpha}(S)}; \quad (11)$$

which is closely related to the topological entropy function. Notice that $M(\alpha)$ measures the relative "volume" of the set with two preimages, $\mu_{\alpha}(E_2)$.

The right hand side of (11) can be interpreted asymptotically as,

$$M(\alpha) \approx \frac{U_n}{T_n} = \frac{U_n}{T_n}; \text{ for large } n; \quad (12)$$

where U_n is the total length of the S_n in $(4\alpha; 1 - \alpha)$, while T_n represents the total length of the S_n in X . For each finite n , $U_n = \mu_{\alpha}(S_n \setminus (4\alpha; 1 - \alpha))$ and $T_n = \mu_{\alpha}(S_n \setminus X)$, can be calculated numerically as the sum of the lengths of subintervals A_{nk} , from Eq. (4). Numerical evidence indicates that the sequence of M_n converges in the limit $n \rightarrow \infty$, at least for almost all (w.r.t. Lebesgue) α . However, for certain values of α , this is not true. For example, for $\alpha = 1/6$ the sequence M_n does not converge, since $M_{2n} = 1/3$ and $M_{2n+1} = 1/2$ for $n = 0; 1; 2; \dots$. We expect that such problems are "atypical" in that they have Lebesgue measure zero, due to the weak convergence of the measures μ_n to μ_{α} . We also observe that, in general, the convergence occurs faster for smaller values of α .

Similarly, the value of $M(\alpha)$ can be expressed by a ratio of natural measures of two intervals:

$$M(\alpha) = \frac{s_{\alpha}([4\alpha; 1 - \alpha])}{s_{\alpha}([2\alpha; 1 - \alpha])}; \quad (13)$$

since the unknown proportionality constant c , mentioned in Remark 1, is eliminated due to cancellation.

We now establish a function which gives the topological entropy $h_T(\alpha)$ of the tent gap-map, in terms of $M(\alpha)$. Therefore, $h_T(\alpha)$ is easily approximated, which may be considered surprising, given that $h_T(\alpha)$ is a "devil's staircase."

Proposition 1: The topological entropy $h_T(\theta)$ of the tent map with θ -gap equals,

$$h_T(\theta) = \ln[1 + M(\theta)] \tag{14}$$

Sketch of the proof [26]: Consider the Ruelle-Bowen transfer operator L , associated with the mixing dynamical system f , which acts on a continuous density function $g : X \rightarrow [0;1]$

$$L[g(x)] = \int_{y \in f^{-1}(x)} g(y) dy \tag{15}$$

found in Ruelle's Perron-Frobenius Theorem, [27]. When θ is a binary rational, (computers can only store such numbers), then there is a conjugacy of f to a subshift of finite type, which is exactly a topological Markov chain, for which Bowen's version of Ruelle's Perron-Frobenius Theorem is stated. If θ is not a binary rational, the conclusion of the theorem still holds [26].

The conclusion is therefore as follows. The operator L has the eigenfunction $\mu(x)$, $L(\mu) = \lambda \mu$, and the adjoint operator L^* has the eigenmeasure ν , $L^*(\nu) = \lambda \nu$ which may be normalized so that $\nu(X) = 1$; both $\mu(x)$, and ν correspond to the same largest eigenvalue λ , and the maximal entropy measure is uniquely absolutely continuous with respect to ν by the density function $\mu(x)$. Thus $d\nu(x) = \mu(x)d\nu(x)$. The topological entropy of f is equal to the logarithm of this largest eigenvalue, λ , of L and L^* [27].

For the model Eq. (1), there is constant slope $|f^0| = 2$, and therefore, for arbitrary n , any normalized uniform measure $\mu_n(X) = 1$ from Eq. (7) iterates,

$$L[\mu_n] = 2\mu_{n+1} \tag{16}$$

where $\mu_n = \frac{1}{2} + M_n$, and μ_{n+1} is also uniform. Therefore, in the weak limit $n \rightarrow \infty$, we obtain $L[\mu] = 2\mu$. Thus, the measure μ is equal to the uniform measure μ_u , and both are absolutely continuous to the maximal entropy measure μ .

The measure of the entire space X with respect to $L(\mu)$ is given by

$$L(\mu)(X) = \mu(E_1) + 2\mu(E_2) \tag{17}$$

since, by definition, for any $x \in E_2$ there exist two preimages $f^{-1}(x) \in S$, and for any $x \in E_1$ there exist only one such preimage. Making use of the eigenequation, $L(\mu) = \lambda \mu$, and the normalization condition $\mu(E_1) + \mu(E_2) = 1$ we arrive at

$$\lambda = 1 + 2\mu(E_2) \tag{18}$$

which proves the formula (14), making use of our special case result that $\mu = \mu_u$.

4 Direct approximation of the topological entropy function

In this section, we give numerical and graphical evidence as to the accuracy of Proposition 1.

Example 1: For $\theta = 1/7$ the continued fraction expansion of (several) numbers M_n consists of ones only, and the sequence M_n converges to the golden number: $M(\theta = 1/7) = \frac{\sqrt{5} + 1}{2} = 1.618034$, so that $h_T(\theta = 1/7) = \ln[(\frac{\sqrt{5} + 1}{2})^2] = 0.481212$.

Example 2: We now consider a sequence of closed form approximates to the devil's staircase entropy function $h_T(\theta)$, based on Eqs. (12)-(14). As the zero order approximation of M , we take the ratio between Lebesgue measures $M_0 = (1 - \theta^4)/(1 - \theta^2)$. Substituting this into (14) gives for $\theta \in [0;1=5]$ an analytical approximation of the entropy

$$h_0(\theta) = \ln \frac{8\theta^4}{1 - 3\theta^2} \text{ for } \theta \in [0;1=5] \tag{19}$$

represented in Fig. 2 by a thin solid line. This formula gives the asymptotic behavior $h_T(\epsilon) \sim \ln 2 - \epsilon$, valid for small ϵ .

Example 3: Calculating higher order ratios M_n yields better approximations for the topological entropy function. For example, M_1 gives

$$h_1(\epsilon) = \begin{cases} \ln[(2 - 10\epsilon) / (1 - 4\epsilon)] & \text{for } \epsilon \in [0; 1/9] \\ \ln[(3 - 11\epsilon) / (2 - 8\epsilon)] & \text{for } \epsilon \in [1/9; 1/7] \\ \ln[(2 - 9\epsilon) / (1 - 4\epsilon)] & \text{for } \epsilon \in [1/7; 1/5] \end{cases} \quad (20)$$

while the next approximation, based on M_2 , reads

$$h_2(\epsilon) = \begin{cases} \ln[(2 - 12\epsilon) / (1 - 5\epsilon)] & \text{for } \epsilon \in [0; 1/17] \\ \ln[(7 - 31\epsilon) / (4 - 20\epsilon)] & \text{for } \epsilon \in [1/17; 1/15] \\ \ln[(4 - 23\epsilon) / (2 - 10\epsilon)] & \text{for } \epsilon \in [1/15; 1/9] \\ \ln[(5 - 19\epsilon) / (3 - 11\epsilon)] & \text{for } \epsilon \in [1/9; 1/7] \\ \ln[(4 - 20\epsilon) / (2 - 9\epsilon)] & \text{for } \epsilon \in [1/7; 2/11] \end{cases} \quad (21)$$

The $h_1(\epsilon)$ and $h_2(\epsilon)$ approximates can also be found in Fig. 2, and we see that $h_2(\epsilon)$ is already pretty good. The solid thick line represents $h_{10}(\epsilon)$, obtained with the uniform measure supported on the set S_{10} , by numerically computing the ratio M_{10} , according to Eq. (12). Crosses denote exact results, computed by roots of polynomials, as described in Appendix A, for values of ϵ corresponding to periodic orbits of length $L = 6$. When $\epsilon < 1/7$, these results coincide to within 10^{-5} . On the other hand some discrepancies are visible for larger gaps, for which convergence of the sequence M_n is slower.

Conjecture: Iterating this procedure produces continuous, piecewise differentiable functions $h_n(\epsilon)$ which, in the limit $n \rightarrow \infty$, converge to the topological entropy versus noise gap function $h_T(\epsilon)$. Convergence is in the L^1 norm, and $\int_0^1 h_T(\epsilon) d\epsilon = \int_0^1 h_n(\epsilon) d\epsilon \rightarrow 0$ as $n \rightarrow \infty$.

5 Structure of the entropy devil's staircase

In fact, Eqs. (12)–(14) of Proposition 1, together with the closed form representation of $A_{m,k}$, found in Eq. (4) can be used to investigate the structure of the devil's staircase topological entropy function, $h_T(\epsilon)$, which we do in this section.

Our primary remark of this section follows from the observation that the function $M(\epsilon)$ is constant for $\epsilon \in [f^{-1}(4^{-m}) - 4^{-m} A_{m,k}, f^{-1}(4^{-m})]$ (for any m and k), since varying the parameter ϵ both integration borders sweep the empty region of X and the measure $\nu(\epsilon)$ does not change in each of these intervals. This is equivalent to an alternative topological description of the same phenomenon: when word bins overlap, no change takes place to the topological entropy of the corresponding symbol dynamics, which must be a subshift of finite-type [13]. In other words, varying the parameter ϵ in these regions does not influence the set of periodic orbits, and hence the topological polynomials [15], or dynamical zeta functions [28], are unchanged and therefore lead to the constant topological entropy.

The condition that the integration sweeps a gap when $\epsilon \in [f^{-1}(4^{-m}) - 4^{-m} A_{m,k}, f^{-1}(4^{-m})]$, defined in (4), gives

$$M(\epsilon) = \text{const} \quad \text{for } \epsilon \in [f^{-1}(4^{-m}) - 4^{-m} A_{m,k}, f^{-1}(4^{-m})] \quad (22)$$

for each m -pre-iteration of the gap (word-length m) ($m = 0; 1; 2; \dots$ and each m -bit word, $k = 1; 2; \dots; 2^m$).

In particular, we have monotonicity of the $M(\epsilon)$ function, and so it must follow that

$$M(\epsilon_1) \geq M(\epsilon_2) \quad \text{for } \epsilon_1 > \epsilon_2: \quad (23)$$

It therefore immediately follows that topological entropy $h_T(\mu)$ is a non-increasing function of μ , as was proven in [14].

Example 4: The gap $A_{0,1}$ generates the main plateau of the "devils staircase" $B_{0,1} = [1=9;1=7]$, for which the topological entropy is equal to $\ln\left(\frac{1}{5} + 1\right) = 2$ – see Example 1 above.

Remark: Inside the main plateau $B_{0,1} = [1=9;1=7]$ all three of the approximate functions, $h_0(\mu)$, $h_1(\mu)$ and $h_2(\mu)$, cross at $\mu = \frac{6}{5} = 31.0121417$, for which the sequence M_n is constant and equal to the golden mean ϕ , corresponding to the exact value of the entropy $h_T = \ln(1 + \phi)$. See Fig. 2.

6 Kneading sequences and the entropy plateaus

The kneading theory of Milnor and Thurston [15] allows us to compute the topological entropy of a unimodal map from the orbit of its critical point, using the so-called kneading determinant (see e.g. [29]). This technique may also be applied in our analysis of the tent map with a symmetric gap, for which the critical orbit originates in one of (either) two ends of the gap: $[(1-\mu)=2; (1+\mu)=2]$. It enables us to express the topological entropy for any μ at steps of the staircase, $\mu \in B_{m,k}$, as

$$h_T(\mu_{m,k}) = \ln(\lambda_{m,k}); \quad (24)$$

where $\lambda_{m,k}$ is the largest (real) root of the polynomial $P_a(z)$ of order $m+2$,¹ which is the characteristic polynomial of the Stefan transition matrix [30]. As shown in Appendix A, all of the coefficients $\{c_{m+2}; c_{m+1}; \dots; c_1; c_0\}$ are equal to either $+1$ or -1 . These coefficients are uniquely determined by the kneading sequence, representing the symbolic itinerary of a periodic critical orbit. It follows, from Eq. (24), that the values of the corresponding plateau $B_{m,k}$ in the space of μ , are also uniquely determined by these same coefficients.

We remark that for the polynomials $P_a(z)$ are closely related to the kneading determinant $P_a(z)$ of Milnor and Thurston. For any plateau $B_{m,k}$, associated with an orbit of the length $L = m+3$, the kneading invariant is proportional to a finite polynomial $P_b(1=z)$ and the topological entropy is given as the logarithm of the smallest root of $P_b(1=z)$ [15, 31]. Kneading determinants are considered a standard tool to compute the topological entropy of one-dimensional maps [32, 33, 17], but for our purposes, we find the related polynomials $P_a(z)$ are more convenient.

To highlight our understanding of the relationship between the function $h_T(\mu)$, displayed in Fig. 2, relative to calculations based on Eq. (24), we have constructed Table 1, by collecting the kneading sequences, corresponding polynomials, their largest roots, and the values of the topological entropies for plateaus corresponding to periodic orbits. Each plateau occurs for $\mu \in [\mu^-; \mu^+]$ given by Eq. (22). The orbits of length $L = 3$ through 7 (and some of the length $L = 8$) are ordered according to the decreasing entropy, which corresponds to increasing width of the gap μ . Any periodic orbit may represent a kneading sequence, but not vice-versa; some kneading sequences (and hence the corresponding polynomials) are not admissible for the tent map (see e.g. [34, 35]) as they do not correspond to any periodic orbits in the system, and therefore, do not affect the dependence $h_T(\mu)$.

Example 5: Consider the main plateau $B_{0,1} = [1=9;1=7]$. The critical orbit is has the length $L = m+3 = 3$, representing the kneading sequence CRL , corresponding to the sequence of coefficients $\{+\dots\}$, which denotes the polynomial $P_a(z) = z^2 - z - 1$. The symbols C, R, L , are used to mark, whether each iterate is at the critical point (Center), right of it (Right) or left of it (Left). Largest root of the (this) equation $P_a(z) = 0$ equals $\phi_{0,1} = 1 + \phi$ where ϕ denotes the golden mean $\left(\frac{1}{5} + 1\right) = 2$. The one follows the same result for topological entropy discussed in Proposition 1.

¹added line

We characterize a peculiarity in the structure of the devil's staircase, visible in Fig.1, by the following

Proposition 2: Any entropy plateau corresponding to an orbit of length L is accompanied on the left (smaller gap width) by an infinite number of adjacent plateaus with the same entropy, which are caused by orbits of period $2L, 4L, 8L, \dots$.

To prove this proposition, consider the sequence of signs $[c_{L-1}; c_{L-2} \dots; c_1; c_0]$, (denoting a polynomial corresponding to an orbit of length L , as mentioned above). Also consider the following operations acting on the sequences of signs $c_i = \pm 1$ of length L , which double their length:

$$W_1 [c_{L-1}; c_{L-2} \dots; c_1; c_0] = [c_{L-1}; c_{L-2} \dots; c_1; c_0; c_{L-1}; c_{L-2} \dots; c_1; c_0]; \quad (25)$$

$$W_2 [c_{L-1}; c_{L-2} \dots; c_1; c_0] = [c_{L-1}; c_{L-2} \dots; c_1; c_0; c_{L-1}; c_{L-2} \dots; c_1; c_0]; \quad (26)$$

In a straightforward way, these transformations, discussed in [15], may be mapped into the space of polynomials, of order $L-1$, with all coefficients equal to ± 1

$$W_1(P_a(z)) = (z^{L-1} - 1)P_a(z); \quad W_2(P_a(z)) = (z^{L-1} + 1)P_a(z); \quad (27)$$

Since the roots of the factor $(z^{L-1} - 1)$ are situated on the unit circle, the largest real roots of the polynomial $P_a(z)$, and its two images, $P^0 = W_1(P_a(z))$ and $P^{\infty} = W_2(P_a(z))$, are the same. Therefore, if there exist admissible periodic orbits corresponding to the "descendent" polynomials P^0 and P^{∞} , then they form a plateau of the same height as their "ancestor" polynomial.

We find, in fact, that there are such plateaus corresponding to the descendants P^0 , but not for the descendants P^{∞} . We establish, in a somewhat indirect way, the existence of the P^0 plateaus by considering their location (terminology as used in [34]). Let us rewrite, in a simplified form, the position of the plateau induced by the polynomial according to Eq. (22): $B_{L,j} = [j=(2^L + 1); j=(2^L - 1)]$, where $L = m + 3$ and $j = 2k - 1$. Using the fact that the sequence of coefficients c_i represent the integer $k - 1$ in the binary code (but not the itinerary code: see Appendix A), we arrive at the conclusion that the polynomial P^0 is associated with the plateau $B^0 = B_{2L,j^0}$, where $j^0 = j(2^L - 1)$. Therefore, this descendent plateau $B^0 = [j(2^L - 1)=(2^{2L} + 1); j(2^L - 1)=(2^{2L} - 1)(2^L + 1)]$ touches, from the left, the ancestor plateau $B_{L,j} = [j=(2^L + 1); j=(2^L - 1)]$ and thus induces the devil staircase. This reasoning is valid for any admissible periodic orbit of length L . Since the descendent plateau, corresponding to the orbit of length $2^n L$, has descendants related to the orbit of the length $2^{n+1} L$, there exists an infinite sequence of plateaus (related to the orbits of length $2^n L, n = 1; 2; \dots$) and Proposition 2 is justified. Furthermore, the length of these adjacent plateaus, determined by the denominators $2^n L$, decreases exponentially with n , and their total sum gives the total width of a plateau.

The "would-be" P^{∞} plateaus may be formally constructed, but we find that they are entirely included within the boundaries of the ancestor plateaus. In the analogous construction to that of the previous paragraph, we find that the polynomial P^{∞} would be associated with plateau $B^{\infty} = B_{2L,j^{\infty}}$, where $j^{\infty} = j(2^L + 1)$. Calculating the location, $B^{\infty} = [j(2^L + 1)=(2^{2L} + 1); j=(2^L + 1)]$, we see that its right edge coincides with the right edge of the plateau $B_{L,j}$. I.e., $B^{\infty} \subset B_{L,j}$. Consequently, descendants P^{∞} are entirely shadowed by the longer ancestor plateaus and do not affect the devil staircase. This reflects the fact that the sequences P^{∞} do not correspond to any admissible periodic orbits (see eg. [35], pp. 136-139).

Example 6: The golden plateau $B_{0,1}$, with $l=2$ $[l=9; 1=7]$ found by Eq (22), is represented by the polynomial $P = [t \dots]$, according to Eqs. (39)-(40), using $m = 0, k = 1$ and $L = m + 3 = 3$. The two descendant polynomials are $W_1(P) = P^0 = [t \dots + +]$ and $W_2(P) = P^{\infty} = [t \dots + \dots]$. The former represents the orbit $CRLRL$ leading to the plateau for $l=2$ $B_{3,4} = [7=65; 7=63]$ (again by Eqs. (22) and (39)-(40), which forms an extension of the "golden" plateau $[l=9; 1=7]$ of the same entropy $\ln(1 + \frac{1}{2})$. The latter corresponds to the non-admissible orbit $CRLRL$ [32] and the hidden plateau $B_{3,5} = [9=65; 9=63]$ which is a subset of the golden plateau. Existing left extensions of shorter orbits plateaus are marked by "E" in the Table 1, and for pedagogical purposes, we also include the non-existing hidden plateaus (stemming from polynomials P^{∞}) marked by the letter "N".

In order to analyze the case of wide ϵ -gaps, characterized by a decreasing entropy, it is helpful to consider two other operations doubling the sequences of signs

$$U_1 [c_{L-1}; c_{L-2} \dots; c_1; c_0] = [c_{L-1}; c_{L-1}; c_{L-2}; c_{L-2} \dots; c_1; c_1; c_0; c_0]; \quad (28)$$

$$U_2 [c_{L-1}; c_{L-2} \dots; c_1; c_0] = [c_{L-1}; c_{L-1}; c_{L-2}; c_{L-2} \dots; c_1; c_1; c_0; c_0]; \quad (29)$$

and the corresponding transformations in the space of polynomials

$$U_1 (P_a(z)) = (z-1)P_a(z^2); \quad U_2 (P_a(z)) = (z+1)P_a(z^2); \quad (30)$$

Let ρ denotes the largest root of the polynomial of order $L-1$. It is easy to see that the largest roots of the descendent polynomials $p_3 = U_1(\rho)$ and $p_4 = U_2(\rho)$ of order $2L-1$ are equal to $\sqrt{\rho}$, so the corresponding entropies are halved. The sequences p_4 do not correspond to any of the admissible periodic orbits [35], and the operator U_2 is mentioned here for completeness only. On the other hand, a renormalization operator U_1 , generating admissible periodic orbits p_3 , is often discussed in the literature [32, 35, 17]. In a natural way this operator can be generalized to act in the space of infinitely long sequences. The corresponding operation of the kneading sequences, which doubles the length of the periodic orbit, is a special case of the Devillard-Gervois-Pompeu composition [30].

Remark: We are now in a position to bound the critical last gap value ϵ , for which any larger ϵ -gap has no topological entropy, since all of the gaps have overlapped. This remark is summarized by Fig. 3. The tent map with no gap ($\epsilon = 0 = 0$) is characterized by the kneading sequence $Q = CR(L)^1$, polynomial $p_0 = [t \dots]$ and the entropy $\ln 2$. The kneading sequence $R^*Q = CRL(R)$ is represented by the polynomial $U_1(p_0) = [t \dots + (\dots)^1]$. Consequently, the entropy $\ln 2 = 2$ is achieved for $\epsilon = \epsilon_1 = 1 = 6$. In this way we construct a family of kneading sequences $R^{n*}Q$ and the polynomials $U_1^n(p_0)$, which allow us to find the sequence of numbers ϵ_n such that $h_T(\epsilon_n) = 2^n \ln 2$. In particular $\epsilon_2 = 7 = 40 = 0.175$, while already the next value $\epsilon_3 = 0.175092$ provides a good approximation of the Feigenbaum critical point $\epsilon = \lim_{n \rightarrow \infty} \epsilon_n$.

The same value can be approached from above by considering wider gaps $\epsilon > \epsilon_1$, corresponding to periodic orbits of the length $L = 2^1$, which lead to the zero entropy. A gap of the width $\epsilon = \epsilon_1 = 1 = 5$ leads to the orbit $S = CR$ and a trivial polynomial $p_1 = [t \dots]$ with the root $\rho = 1$. For this polynomial both operations W_1 and U_1 produce the same result $p_2 = [t \dots + \dots]$ (since half of zero entropy is equal to zero). The corresponding orbit CLR appears at $\epsilon = \epsilon_2 = 3 = 17 = 0.17647$. Subsequent processes of period doubling occur at the gaps $\epsilon = \epsilon_n$ corresponding to the polynomials $p_n = U_1^n(p_1)$. For example $p_3 = [t \dots + \dots + \dots]$ gives $\epsilon_3 = 45 = 257 = 0.175097$, where $L = 8, m = L - 3 = 5, k = 2j + 1 = 45, j = 22$, and $2^L + 1 = 257$ are all consistent, again by Eqs. (22) and (39)-(40). In general

$$\epsilon_n = \frac{1}{2^{2^n} + 1} \prod_{k=0}^{n-1} (2^{2^k} + 1); \quad (31)$$

and each zero entropy plateau $\epsilon \in [\epsilon_{n+1}; \epsilon_n]$ forms an extension of the plateau $[\epsilon_n; \epsilon_{n-1}]$.

The sequence ϵ_n converges quadratically $((\epsilon_{n+1} - \epsilon_n) / (\epsilon_n - \epsilon_{n-1}))^2$, in contrast with the geometric convergence of the well known Feigenbaum sequence $((\epsilon_{n+1} - \epsilon_n) / (\epsilon_n - \epsilon_{n-1})) = \delta$, asymptotically as the Feigenbaum delta constant), which describes the period doubling in the logistic map [23]. The first 15 decimal digits of ϵ_5 and ϵ_6 are the same and provide an excellent approximation of the Feigenbaum point,

$$\epsilon = 0.17509193271978; \quad (32)$$

This can be considered as a sharp estimate for the maximal topologically nondegenerate gap. A sketch of the behavior of the function $h_T(\epsilon)$ in the vicinity of the critical point ϵ is shown in Fig. 3.

Previous attempts to calculate the critical last gap ϵ , by "brute-force" direct computation of the topological entropy (by counting symbol sequences) on the invariant set, break-down due to the exponentially

increasing difficulty (see conjecture associated with Eq. (36) of locating the ever thinning invariant set (by PIM triple method) [13]. For the first time, we can now draw the curve all the way to zero entropy, as shown in Fig. 3.

Remark: The analyzed structure of the dependence of the topological entropy is typical for all unimodal maps with a gap. While location of the entropy plateaus depends on the map and on the position of the gap, the heights of the plateaus are universal. The same sequences of entropy plateaus occurs for some 1D maps without the gap. For example, the periodic windows for the logistic map are characterized by zero (or negative) KS-entropy and a constant topological entropy. Its value is determined just by the kneading sequence of the periodic orbit and therefore, can be expressed by roots of the polynomials discussed in this work. A figure of parametric dependence of the topological entropy for quadratic map (related with logistic map) is already sketched in the preprint of Milnor and Thurston [15], and a more precise picture of such dependence is presented in the review of Eckmann and Ruelle [16] and in the paper by Gora and Boyarsky [36].

7 Topological Entropy is the "Average" Pre-Image Count

In this section, we pursue a result, suggested by part of the proof of Proposition 1. For a more general map than the (constant slope) tent map, we do not have the coincidence of uniform measure μ and the Parry measure ν , and therefore we cannot conclude Eq. (16) with a uniform m_n . Nonetheless, we can make the following general Proposition,

Proposition 3: The topological entropy of a 1D mixing system $f : X \rightarrow X$, for a piece-wise monotone function f , which is continuous on the N branches, is equal to

$$h_T = \ln \int_X P(x) d(x); \quad (33)$$

where $P(x) : X \rightarrow \{0; 1; 2; \dots; N\}$ represents the number of preimages of f at the point x (restricted to the support of μ) and the average is taken with respect to the Lebesgue measure μ , which is absolutely continuous to the maximal entropy measure μ by the Lebesgue density $d(x)$.

Note that one cannot generally expect $P(x)$ to be surjective, onto the set $\{0; 1; 2; \dots; N\}$.

Proof: The proof is very similar to the second half of the proof of Proposition 1, which is all that survives the weaker condition, that we allow maps with arbitrary slopes. As before, we split X into $X = \bigcup_{j=0}^N E_j$, where $E_j = \{x \in X : f^{-1}(x) \text{ has } j \text{ branches}\}$. The adjoint eigenstate equation of the Bowen transfer operator L , measuring the whole space X , is

$$L^*(\psi) = \sum_{j=0}^N \int_{E_j} \psi(f(x)) d(x) = \langle P(x) \rangle = \left\langle \frac{P(x)}{\mu(x)} \right\rangle; \quad (34)$$

where, as before, the eigenmeasure of the operator L , μ , is known to be uniquely absolutely continuous to Parry's maximal entropy measure μ , by $d(x)$, which is the eigenfunction of the adjoint eigenequation $L^* \psi = \lambda \psi$. Therefore, the eigenvalue of this equation is $\lambda = \langle P(x) \rangle$, and the topological entropy is, $h_T = \ln(\langle P(x) \rangle) = \ln \left\langle \frac{P(x)}{\mu(x)} \right\rangle$. 2

Example 7: Take any unimodal map with a.e. 2 preimages, such as the logistic map, $x^0 = 4x(1-x)$ which is well known [23] to have topological entropy $h_T = \ln(2)$, when the parameter value $a = 4$. This result is particularly easy to derive by Proposition 3, for which we may check that, $h_T = \ln(\langle P(x) \rangle)$

$) = \ln \binom{R}{[0;1]2d} = \ln \binom{R}{[0;1]d} = \ln 2$, as expected. The main simplifying feature of the calculation is that only the number of branches, weighted by the normalized measure, was important, and thus the calculation is quite general (and hence identical for, say, the two-onto-one tent map, the two-onto-one cusp map, etc.).

We note that our formula Eq. (34) is reminiscent to a similar formula, for almost all x , $h(f) = \lim_{n \rightarrow \infty} \frac{1}{n} \log \# f^n(x)$, used in Lopes and Wither's [37]. The link follows by considering their formula as an average of the number of pre-images, of the initial condition, in which some branches are presumably dense in X , which is just the same as using the measure of maximal entropy.

8 Fractal Dimension and Escape Rate

So far, we have only considered the topological entropy. The so-called "at-spots" of the topological entropy function, caused by overlapping symbolbins, which causes the integral of Eq. (11) for $(M(\epsilon))$ to "sweep a gap" when $\epsilon \geq \epsilon^*$: A_{mk} defined in (4), also has consequences to the spectrum of pointwise spectrum of Renyi-Dimensions D_q [38] (see e.g. [23] pp 79, or pp 306 for review). We now discuss these implications in this section.

We conjecture that the Hausdorff dimension of the support S (and the measure μ) coincide with all of the generalized Renyi (multifractal) dimensions D_q [23], and hence we write

$$D_0 = D_q = \frac{\ln(1+M)}{\ln 2} \quad (35)$$

In [22], we find the relationship $D_1 = h_{KS} = \ln 2$, directly linking the information dimension proportionally to the KS entropy, and this corresponds to the Kaplan-Yorke conjecture [23], formulated in a different setting. The dimension is thus proportional to entropy and displays the same devil staircase like dependence on the parameter ϵ .

Next we consider the nature of this map as a dynamical system on the unit interval, whose invariant set is an unstable chaotic saddle. Therefore, the initial conditions which are not on this invariant set, escape to infinity. In the analogy to [22, 25], we conjecture that iterating f_ϵ , on an initially uniform measure, causes the mass of points to decay exponentially with the number of iterations, according to $\exp(-Rn)$. From such an exponential decay model follows the exponent R ,

$$R = \ln 2 - h_{KS} = \ln \frac{2}{1+M} \quad (36)$$

Furthermore, this escape rate R describes the exponential convergence of the series M_n , in Eq. (12). Note that the number $M(\epsilon)$, in Eq. (11), defines the limit of this sequence, as well its convergence rate.

There is a striking similarity between the topological entropy devil's staircase function of f_ϵ , and the similar devil's staircase topological entropy of the logistic map $f_r = rx(1-x)$ on the parameter r [17, 39]. This follows immediately from the fact that in both models, we are monotonously nonincreasing the kneading sequence, with the parameters ϵ and r respectively. However, in the case of the tent gap-map f_ϵ , the set G of ϵ values which are not contained in the "at steps" B_{mk} is of zero Lebesgue measure [14] and has a fractal structure [25]. In contrast, the set of r values which lead to chaotic motion (not contained in the "periodic windows" of a constant topological entropy) has a positive Lebesgue measure [40].

It is natural to investigate the homogeneity and the local pointwise dimension D_1 of the set $G \subset [0; \infty)$ of ϵ values not contained in the "at steps" B_{mk} . Consider a fixed value of ϵ and a set S of dimension D_1 which supports the invariant measure $\mu(\epsilon)$ of the system. We perturb the size of the gap, $\epsilon^0 = \epsilon + \delta$, and we find that in the limit $\delta \rightarrow 0$ the measure $\mu(\epsilon^0)$ converges weakly to $\mu(\epsilon)$. As we have already discussed that Eq. (14) of Proposition 1 implies that entropy changes only if the integral (11) changes, which occurs as the integration borders sweep across the fractal set S , but not when we sweep the gaps S .

Therefore we conjecture that the set G is nonhomogeneous and its local point dimension D_1 depends on the size of the gap according to [25],

$$D_1(G(\mu)) = D(\mu) = \frac{\ln(1 + M(\mu))}{\ln 2} : \quad (37)$$

Remark. The intervals $I_n = [x_n; x_{n+1}]$ are similar in the sense that any plateau in the interval I_0 , associated with the polynomial f , has a corresponding plateau in each of the intervals I_n and these descendent plateaus are represented by polynomials $U_1^n(f)$.

Example 8. An orbit $CRLRRR$ is associated with the polynomial $f(x) = x^2 + x + 1 = U_1(f)$, so the corresponding plateau is localized in I_2 and its entropy is equal to $[\ln(1 + \frac{1}{2})] = 2.0240606$. Another descendent plateau, determined by $U_1(f)$, and corresponding to the orbit of the length 8, is marked in Table 1 by the letter 'D'.

Despite the similarity emphasized above, the entropy devil's staircase is not self-similar in the intervals I_n . It is not possible to linearly rescale the interval I_n by a constant factor to get the dependence $h_T(\mu)$ in the next interval I_{n+1} . This corresponds to the fact that the set G is not homogeneous and its local dimension varies with μ .

Remark. The number I_L of plateaus generated by periodic orbits of the length L in the first interval I_0 are listed in Table 2. We do not count those orbits, which produce plateaus embedded in longer plateaus generated by shorter orbits. The column T_L represents the total width of all plateaus generated by all orbits of the length L , while the last column W_L represents the total volume of the parameter space in I_0 not contained in the sum of the plateaus T_L . A naive exponential fit gives $W_L = a + be^{cL}$ with a positive $a = 0.03$, but if G is indeed a fractal contained in the interval, then this approximation can not be true since a should be zero. Comparison with a similar table obtained for logistic map [39] shows that the number of L steps in the entropy dependence on the parameter, which correspond to periodic orbits of a fixed length, are almost the same. On the other hand, the relative Lebesgue measure of the plateaus in the parameter space is much smaller for the logistic map.

9 Pragmatic Conclusions

We have performed a detailed measure theoretic based analysis of the devil's staircase topological entropy function of the gap-tent map whose invariant set is an unstable chaotic saddle invariant set of the tent map. The point was to further analyze the trade-off between channel capacity and noise-resistance in designing dynamical systems to pursue the idea of communications with chaos. One may reduce the effects of an external noise by introducing a gap into the system (i.e. by not using parts of the phase space close to the partition lines). We explicitly demonstrate that some levels of noise are better than others for this purpose. For the simple tent-gap map model system (2x tent map) the noise gap $\mu = 1/7$ provides the same maximal information transmission rate (topological entropy) as the gap $\mu = 1/9$ and offers 128% larger immunity against noise. In general, for this system the gaps $\mu = (2k - 1)/(2^{m+3} - 1)$ (at the right edges of the plateaus B_{mk}), are more useful than when $\mu = (2k - 1)/(2^{m+3} + 1)$ (at the left edges of the plateaus), with fixed natural numbers m and k . Our analysis can also be applied to investigate the effects of noise in measurements performed by electronic devices, in which the result of measurement is determined by a symbolic sequence describing a chaotic trajectory [41].

We would like to mention, in Appendix B, a brief description for our future research, by which the measured statistical properties of deterministic dynamical systems are linked to an appropriately chosen stochastic system by the so-called iterated function systems theory.

Acknowledgments

We are indebted to M. Misiurewicz for a particularly helpful hint leading to the proof of Proposition 1. We also thank Y. Jacobs, B. Hunt, D. Lathrop, M. Ogorzalek, E. Ott, T. Kapitaniak, W. Słomczyński, E. Walters, J.A. Yorke and G.-C. Yuan for helpful discussions. K.Z. acknowledges the Fulbright Fellowship and a support by Polish KBN grant no. P 03B 060 13. E.B. is supported by the National Science Foundation under grant DMS-9704639.

Appendix: Kneading sequences and polynomials for the gap tent

map

If the trajectory of the critical point is periodic the topological entropy of the gap tent map f_n can be expressed as a logarithm of largest root of some polynomial, with all coefficients equal to 1. Even though this fact follows from the kneading theory of Milnor and Thurston [15], we give here a brief derivation of this result and introduce the polynomials and notation used in this paper.

Our reasoning is based on the fact that two conjugate maps share the same topological entropy [23]. For the map f_n (or for other unimodal maps) it is sufficient to find such a value of the slope s of the tent map $f_s(x) := s(1-2|x-1/2|)$, that the kneading sequences are identical. Then the entropy of the analyzed map is equal to $\ln s$ – the entropy of f_s [29]. For the simple orbit CR of length 2 the condition $f_s^2(1/2) = 1/2$ leads to following equation $s(1-s)=1/2$. It can be rewritten as $(s-1)P_2(s) = 0$, with $P_2(s) = (s+1)$ represented by [+].

Proceeding inductively, we assume that a sequence Q of length L corresponds to the polynomial $P_L = [c_{L-1}; \dots; c_1; c_0]$. Extending the kneading sequence by one symbol, $Q \rightarrow QX$, the descendent polynomial $P_{L+1}(s)$ reads

$$P_{L+1}(s) = \begin{cases} sP_L(s) + 1; & \text{for } X = L \\ sP_L(s) + 1; & \text{for } X = R \end{cases} \quad (38)$$

Therefore, every coefficient of any polynomial is equal to 1. Since multiplication of all coefficients of a given polynomial by -1 does not influence its roots, we can arbitrarily define the leading coefficient, c_{L-1} , to be +1. This corresponds to the initial symbol C (strictly speaking it should be L for left end of the plateau and R for the right one). The next sign of the polynomial is determined by the next symbol of the kneading sequence: when the symbol is an L, the sign is the same as the previous sign, while the sign changes when the symbol is an R. More precisely,

$$c_{L-1} = +1, \text{ and } c_j = \prod_{i=j}^{L-2} g_i, \text{ for } j = 0; \dots; L-2; \quad (39)$$

where $g_i(L) = +1$ and $g_i(R) = -1$ [15]. See several examples collected in Table 1.

Any entropy plateau occurring for $n \geq 2$ $B_{m,k}$ may be related with a concrete periodic orbit. Consider, for example, $n_{m-1} = 1/(2^{m+3} + 1)$, which corresponds to left edges of plateaus B_{m-1} defined in Eq. (22). The orbit starting at $x = 2^{-n_{m-1}}$ is periodic with the length $L = m + 3$, and its kneading sequence reads CRL::L. The corresponding polynomial [42] can be found independently by the companion matrix [42] which is equal to the topological transition matrix of the system $f_{n_{m-1}}$. The largest eigenvalues of the topological transition matrices can be used to find the topological entropy – see eg. [30, 35, 36].

Let us order entropy plateaus $B_{m,j,k}$, corresponding to m -th preimages of the gap A_{10} , according to decreasing entropy. When we increase the gap width n , we decrease the critical point $x_c = (1-n)/2$. Since

the real line is ordered monotonically with the order of kneading sequences [15, 34] (and polynomials), the k -th plateau $B_{m,k}$ corresponds to the k -th periodic orbit of the length $L = m + 3$ (ordered according to decreasing entropy). In other words, the periodic orbit represented by the polynomial $[c_{L-1}; c_{L-2}; \dots; c_1; c_0]$ is k -th in the family of orbits of length L , where

$$k = 1 + \sum_{j=0}^{L-2} 2^j (c_j + 1) = 2^L - 1 \quad (40)$$

Thus, this orbit corresponds to the plateau $B_{L-3,k}$, which occurs for the gap sizes, ϵ , determined by Eq. (22) – see Table 1.

B Appendix: Gap-Tent Map and Iterated Function System

We describe here a technique of generating invariant measures for dynamical systems via appropriate IFS as applied in Refs. [44, 45, 46]. In chaos, the initial condition is chosen randomly, albeit in a small ball, (e.g. machine precision in double is typically a ball of radius 10^{-16}), and the sensitive dependence to initial conditions, of the nonetheless deterministic dynamical system, amplifies this randomness. The deterministic chaos problem, can be traded for an appropriately chosen truly stochastic process, which evolves (supposedly exact) initial conditions by a random dynamical system, whose randomness mimics the chaos.

Barnsley's Iterated Function Systems (IFS) [43] are an appropriate formalism by which we may accurately exchange the deterministic problem for the right stochastic problem. In simplest form, an IFS of the first kind involves an iteration $x_{n+1} = F_i(x_n)$, where the function actually used at each step is chosen randomly with place dependent probabilities $p_i(x)g_{i=1}^k$, $\sum_{i=1}^k p_i(x) = 1$, amongst k possible functions $\{F_i(x)g_{i=1}^k\}$.

For the tent gap-map model, we define an IFS consisting of two functions with place dependent probabilities: $F_1(x) = x/2$; $F_2(x) = 1 - x/2$; $p_1 = 0$ for $x < 4\epsilon$ and $p_1 = w$ for $x \geq 4\epsilon$; $p_2 = 1 - p_1$, where the relative weight w is a free parameter. Since there exist points transformed by one function with probability one ($p_2 = 1$ for $x \in [2\epsilon; 4\epsilon]$), the standard assumptions [43, 44] sufficient to prove existence of a unique attracting invariant measure are not fulfilled for this IFS.

Nonetheless we conjecture:

- for every value of $w \in (0;1)$ there exist an attracting invariant measure μ_w of the IFS and it is localized on the same support S as the measure μ_{SRB} .
- for every value of ϵ , there exist $w = w(\epsilon)$ such that the induced invariant measure of the IFS, μ_w , and the SRB measure of the tent map with the gap, are equal: $\mu_{SRB} = \mu_w$.
- the spectrum of entropies K_q and the generalized dimensions D_q for IFS $(\cdot; w(\epsilon))$ and the tent map with a gap ϵ are identical for any fixed value of ϵ .

Let us consider the simplest case with the gap of the width $\epsilon = 1/7$ for which $M = 1/7$ (compare to Example 1). Since the interval $(4/7; 6/7)$ of the mass M is transformed by this IFS, with probability w , into the interval $(2/7; 3/7)$ of mass $1 - M$, the relative weight w is equal to $(1 - M)/M = (1/7)/(1/7) = 1$. More generally, for $\epsilon \geq B_{m,1}$ the above relation is fulfilled for $w = 1 - \epsilon/m$, so in the limit of no gap $\epsilon \rightarrow 0$ one has $\lim_{m \rightarrow \infty} (1 - \epsilon/m) = 1$ and the IFS becomes symmetric ($w = p_1 = p_2 = 1/2$).

References

- [1] R.C. Adler, A.C. Konheim, and M.H. McAndrew, Trans. Am. Math. Soc. 114, 309 (1965).

- [2] C. E. Shannon and W. Weaver, *The Mathematical Theory of Communication*, The University of Illinois Press, 1964.
- [3] R. E. Blahut, *Principles and Practice of Information Theory* (Addison-Wesley, 1988).
- [4] S. Hayes, C. Grebogi, and E. Ott, *Phys. Rev. Lett.* 70, 3031 (1993); S. Hayes, C. Grebogi, E. Ott, and A. Mark, *Phys. Rev. Lett.* 73, 1781 (1994); E. Rosa, S. Hayes, and C. Grebogi, *Phys. Rev. Lett.* 78, 1247 (1997); E. Bollt, M. Dolnik, *Phys. Rev. E* 55, 6404 (1997).
- [5] K. M. Cuomo, A. V. Oppenheim, *Phys. Rev. Lett.* 71, 65 (1993); L. Kocarev, U. Parlitz, *Phys. Rev. Lett.* 74, 5028 (1995); U. Parlitz, L. O. Chua, L. Kocarev, K. S. Halle, A. Shang, *Int. J. Bifur. Chaos* 2, 973 (1992); U. Parlitz, L. Kocarev, T. Stožanovski, H. P. Reckel, *Phys. Rev. E* 53, 4351 (1996); K. Murali, M. Lakshmanan, *Phys. Rev. E* 48, R1624 (1993); C. Zhou, T. Chen, *Phys. Letts. A* 225, 60 (1997).
- [6] E. Ott, C. Grebogi and J. Yorke, "Controlling chaotic dynamical systems", *Chaos: Soviet-American Perspective on Nonlinear Science* (American Institute of Physics, N.Y., 1990) 153-172.
- [7] S. Smale, "Differentiable Dynamical Systems," *Bull. AMS*, Vol 73, 747-817, 1967.
- [8] C. Robinson, *Dynamical Systems: Stability, Symbolic Dynamics, and Chaos*, (CRC Press, Ann Arbor 1995).
- [9] Y. C. Lai, C. Grebogi, J. A. Yorke, and I. Kan, "How often are chaotic saddles nonhyperbolic", *Nonlinearity* 6 779 (1993).
- [10] P. Grassberger, H. Kantz and U. Mosenig, *J. Phys. A* 22, 5217 (1989).
- [11] P. Cvitanovic, G. Gunaratne, and I. Prigogina, *Phys. Rev. A* 38, 1503 (1988).
- [12] E. Bollt, Y.-C. Lai, and C. Grebogi, *Phys. Rev. Lett.* 79, 3787 (1997).
- [13] E. Bollt, Y.-C. Lai, "Dynamics of coding in communicating with chaos," *Phys. Rev. E* 1998, in press.
- [14] K. M. Brucks, M. Misiurewicz, and C. Tresser, "Monotonicity properties of family of trapezoidal maps," *Comm. Math. Phys.* 137, 1 (1991).
- [15] J. Milnor and W. Thurston, *On iterated maps of the interval I and II* Princeton University Press (Princeton, 1977), and J. Milnor and W. Thurston, *On iterated maps of the interval* *Dynamical Systems*, 465-563, *Lecture Notes in Math.* 1342, Springer, Berlin 1988.
- [16] J.-P. Eckmann and D. Ruelle, "Ergodic theory of chaos and strange attractors," *Rev. Mod. Phys.* 57, 617 (1985).
- [17] Z.-X. Chen, K.-F. Cao, and S.-L. Peng, "Symbolic dynamics analysis of topological entropy and its multifractal structure," *Phys. Rev. E* 51, 1983 (1995).
- [18] B. R. Hunt, E. Ott, "Structure in the parameter dependence of order and chaos for the quadratic map," *J. Phys. A* 30, 7067 (1997).
- [19] J. Gaczyk and G. Świątek, "Generic hyperbolicity in the logistic map," *Ann. Math.* 146, 1 (1997).
- [20] R. Haner, R. Schilling, "Pressure dependence of the Number of Metastable Configurations: A Staircase-like Behavior for a Chain of Particles," *Europhys. Lett.*, 8(2), 129-134 (1989); B. Ruckerl, C. Jung, "Scaling properties of a scattering system with an incomplete horseshoe," *J. Phys. A: Math. Gen.* 27 55-77 (1994); P. van der Schoot, M. E. Cates, "The Isotropic-to-Nematic Transition in Semi-Flexible Micellar Solutions," *Europhys. Lett.*, 25(7), 515-520 (1994); W. Breymann, J. Vollmer, "Symbolic dynamics and topological entropy of the onset of pruning," *Z. Phys. B* 103, 539-546 (1997).

- [21] A. Katok, B. Hasselblatt, *Introduction to the Modern Theory of Dynamical Systems*, Cambridge University Press, Cambridge, UK (1995).
- [22] T. Bohr and D. Rand, The entropy function for characteristic exponents, *Physica D* 25, 387 (1987).
- [23] E. Ott, *Chaos in Dynamical Systems*, Cambridge University Press, Cambridge, 1994.
- [24] A. Renyi, "On measures of entropy and information," *Proc. of the Fourth Berkeley Sym. Math. Stat. Prob.* 1960, Vol. I (U. Cal. Press, Berkeley, 1961), pp. 547-561.
- [25] J. Jacobs, E. Ott and B. R. Hunt, Calculating topological entropy for transient chaos with an application to communicating with chaos. *Phys. Rev. E*, 57, 6577 (1998).
- [26] Based on remarks in private correspondence with M. Misiurewicz.
- [27] R. Bowen, *Equilibrium States and the Ergodic Theory of Anosov Diffeomorphisms*, Springer-Verlag, Berlin 1975.
- [28] D. Ruelle, *Statistical Mechanics, Thermodynamic Formalism*, Addison-Wesley, Reading MA.
- [29] W. de Melo and S. van Strien, *One-Dimensional Dynamics*, Springer, Berlin, 1993.
- [30] B. Derriada, A. Gervois, and Y. Pomeau, *Ann. Inst. Poinc. A* 29, 305 (1978).
- [31] J. Guckenheimer, The growth of topological entropy for one dimensional maps, in *Global theory of dynamical systems*, 216-223, *Lecture Notes in Math.* 819, Springer, Berlin 1980.
- [32] P. Collet, J.P. Crutchfield, and J.-P. Eckmann, Computing the topological entropy of maps, *Comm. Math. Phys.* 88, 257 (1983).
- [33] C.S. Hsu and M.C. Kin, Construction of maps with generating partitions for entropy evaluation. *Phys. Rev. A* 31, 3253 (1985).
- [34] Robert L. Devaney *An Introduction to Chaotic Dynamical Systems II ed.*, Addison-Wesley, Reading MA. 1989.
- [35] Hao Bai-Lin *Elementary Symbolic Dynamics*, World Scientific, Singapore. 1989.
- [36] P. Gora and A. Boyarsky, Computing the topological entropy of 1D maps, *Trans. Amer. Math. Soc.* 323, 39 (1991).
- [37] A.O. Lopes and W.D. Witheres, Weight-balanced measures and free energy for one-dimensional dynamics. *Forum Math.* 5, 161 (1993).
- [38] A. Renyi, *Probability Theory*, North Holland, Amsterdam (1970); and for the formulation in the context of chaos theory: P. Grassberger, *Phys. Lett. A* 97, 227 (1983); H.G.E. Hentschel, I. Procaccia, *Physica D*, 8, 435 (1983).
- [39] K.-F. Cao, Z.-X. Chen, and S.-L. Peng, Global metric regularity of the devil's staircase of topological entropy, *Phys. Rev. E* 51, 1989 (1995).
- [40] M.V. Jacobson, *Sov. Math. Dokl.* 19, 1452 (1978).
- [41] M.P. Kennedy, A nonlinear dynamics interpretation of algorithmic A=C conversion, *Int. J. Bifurcation and Chaos* 5, 891 (1995).
- [42] R.A. Horn and C.R. Johnson, *Matrix Analysis* (Cambridge University Press, Cambridge 1990).

- [43] M .F .Bamsley, *Fractals E verywhere* (A cadem ic P ress, B oston, 1988).
- [44] M .F .Bamsley, S.G .D em ko, J.H .E lton, and J.S.G eronim o, Invariant m easures forM arkov processes arising from iterated function system s with place-dependent probabilities. *A nn . Inst. H enriP oincare* 24, 367 (1988); and erratum , *ibid.* 25, 589 (1989).
- [45] P .G ora and A .B oyarsky, Iterated function system s and dynam ical system s. *C haos* 5, 1 (1995).
- [46] W .S lbczynski, J K wapien and K Z yczkowski, M ultifractals and entropy com puting, preprint chaodyn 9804006.

Figure captions

Figure 1 Tent map with an ϵ -gap represented by the central dark strip. Its preimages of the first and second order are represented by narrower vertical strips. The support of the invariant measure can be divided into two parts: E_2 , for which each point has two preimages and E_1 for which there exist only one preimage.

Figure 2 Topological entropy h_T of the tent map as a function of the gap width ϵ obtained via Eq. (14) (thick line). Crosses represent points at the edges of the entropy plateaus computed from roots of polynomials (24). Position of the main plateaus are labeled according to the relation (22). Narrow solid, dashed and dotted lines represent continuous approximations of $h_0(\epsilon)$, $h_1(\epsilon)$, and $h_2(\epsilon)$ respectively, (Eqs. 19 – 21) of the zero-th, first, and second order, respectively.

Figure 3 Sketch of the dependence of topological entropy h_T on the gap width ϵ in the vicinity of the critical point $\epsilon = \epsilon_c$.

Table 1. Topological entropy at plateaus and the corresponding periodic orbits for the tent map $2x$ with symmetric ϵ -gap for $x \in [1 - \epsilon, 1 + \epsilon]$. Subsequent columns contain respectively : length of the orbit L , root r , topological entropy equal to $\ln(r)$, polynomial, number $k \geq 1$ labeling the L -th preimages of the critical point, kneading sequence, both edges of the plateau ϵ_- and ϵ_+ . The symbol $[+]$ represents the polynomial $x^2 - x - 1 = 0$, which root gives the golden mean. The letter E denotes an descendent orbit forming an extension of the plateau related to the two times shorter ancestor orbit, N denotes a non-admissible orbit, which plateau is entirely shadowed by the ancestor plateau. The symbol D represents descendent orbits obtained by the renormalization operation W_1 : two times longer period corresponds to two times smaller topological entropy.

Length		Entropy	Polynomial	k-1	Knearing Seq.	"	" ₊
7	1.9835828	0.6849047	[+ - - - - - -]	0	CRLLLLL	0.00775	0.00787
6	1.9659482	0.6759747	[+ - - - - -]	0	CRLLLL	0.01538	0.01587
7	1.9468563	0.6662159	[+ - - - - - +]	1	CRLLLLR	0.02326	0.02362
5	1.9275620	0.6562560	[+ - - - - -]	0	CRLLL	0.03030	0.03226
7	1.9073421	0.6457107	[+ - - - - + -]	2	CRLLLRR	0.03876	0.03937
6	1.8832035	0.6329743	[+ - - - - +]	1	CRLLLR	0.04615	0.04762
7	1.8558860	0.6183622	[+ - - - - + +]	3	CRLLLRL	0.05426	0.05512
E 8	1.8392868	0.6093779	[+ - - - - + + +]	7	CRLLLRL	0.05837	0.05882
4	1.8392868	0.6093779	[+ - - -]	0	CRLL	0.05882	0.06667
N 8	1.8392868	0.6093779	[+ - - - + - -]	8	CRLLRRL	0.06615	0.06667
7	1.8239445	0.6010015	[+ - - - - -]	4	CRLLRRL	0.06977	0.07087
6	1.7924024	0.5835568	[+ - - - + -]	2	CRLLRR	0.07692	0.07937
7	1.7548777	0.5623992	[+ - - - + - +]	5	CRLLRRR	0.08527	0.08661
5	1.7220838	0.5435351	[+ - - - +]	1	CRLLR	0.09091	0.09677
7	1.6859262	0.5223151	[+ - - - + + -]	6	CRLLRLR	0.10078	0.10236
E 6	1.6180340	0.4812118	[+ - - - + +]	3	CRLLRL	0.10769	0.11111
3	1.6180340	0.4812118	[+ - -]	0	CRL	0.11111	0.14286
N 6	1.6180340	0.4812118	[+ - - + - -]	4	CRLRRL	0.13846	0.14286
7	1.5560302	0.4421378	[+ - - + - - +]	9	CRLRRLR	0.14729	0.14961
5	1.5128764	0.4140127	[+ - - + -]	2	CRLRR	0.15152	0.16129
7	1.4655712	0.3822451	[+ - - + - + -]	10	CRLRRRR	0.16279	0.16535
D 8	1.3562031	0.3046889	[+ - - + - + - +]	21	CRLRRRRR	0.16732	0.16863
D 6	1.2720197	0.2406059	[+ - - + - +]	5	CRLRRR	0.16923	0.17460
DE 8	1.0	0.0	[+ - - + - + + -]	22	CRLRRRLR	0.17510	0.17647
DE 4	1.0	0.0	[+ - - +]	1	CRLR	0.17647	0.20000
2	1.0	0.0	[+ -]	0	CR	0.20000	0.33333

Table 2. Number I_L of periodic orbits of length L creating a plateau in the entropy dependence K (") for $\mu = 0; 1=6$. Total length of these plateaus equals T_L . Cumulative number of plateaus $I_{tot} = \sum_{k=3}^L I_L$, while $W_L = 1 - \sum_{k=3}^L T_L$ represents the total volume of the parameter space not included in the plateaus.

L	I_L	I_{tot}	T_L	W_L
3	1	1	0.03175	0.13492
4	1	2	0.00784	0.12708
5	3	5	0.01759	0.10948
6	3	8	0.00781	0.10167
7	9	17	0.01086	0.09080
8	13	30	0.00659	0.08421
9	28	58	0.00720	0.07701
10	45	103	0.00522	0.07179
11	93	196	0.00528	0.06651
12	161	357	0.00412	0.06238
13	315	672	0.00396	0.05842
14	567	1239	0.00330	0.05512
15	1091	2330	0.00307	0.05205
16	2018	4348	0.00267	0.04938
17	3855	8203	0.00247	0.04692

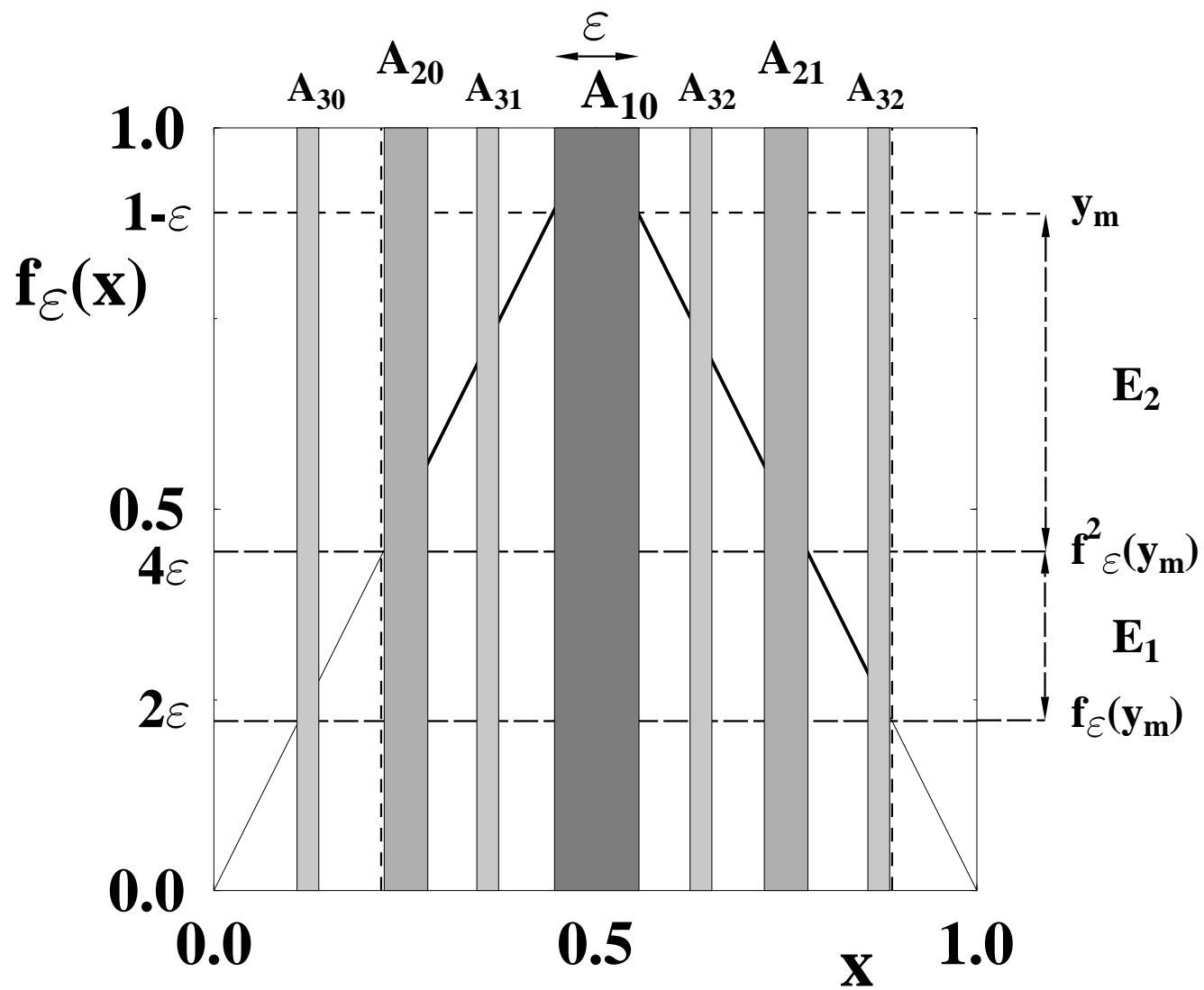


Fig. 1

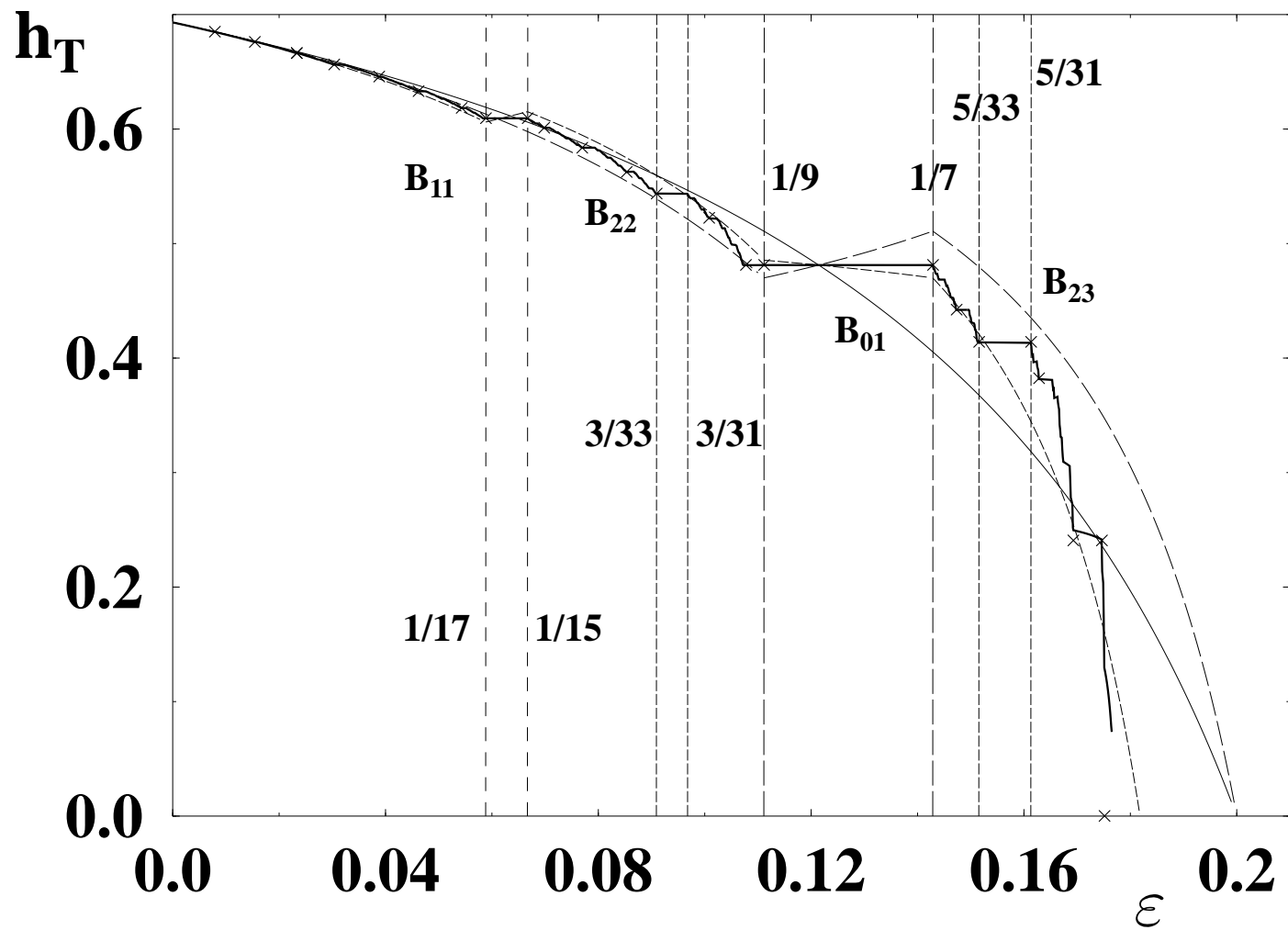


Fig. 2

